

Characterization of Atmospheric Optical Turbulence Using Turbulence Flux Measurements

Alexander M. Peralta*, Charles Nelson, and Cody J. Brownell
United States Naval Academy, Annapolis, Maryland

Abstract

Light propagation through the atmosphere is affected by fluctuations in the refractive index along the path of propagation, called optical turbulence. In the atmospheric surface layer, these fluctuations are due mostly to turbulent mixing of variations in temperature and humidity. To improve understanding and prediction of optical turbulence, a characterization of the atmospheric surface layer above the Severn River is presented. Meteorological data is collected from a sensor array, to include two sonic anemometers and an infrared gas analyzer (IRGASON), located at the Waterfront Readiness Center basin (38.98N, 76.46W) in Annapolis, Maryland. The instruments are positioned vertically at distances up to 8-m over the waterline to analyze boundary layer profiles. The array is arranged to optimize the airflow over the instrument's wicks. Using characteristics such as wind speed, temperature, pressure, and other parameters, the structure parameters for temperature, humidity, and refractive index can be calculated using several different methods. These structure parameters are the primary means of estimating turbulent effects on laser propagation. From field data, assessment of optical turbulence profiles, such as Huffnagel Valley (HV5/7), or constant flux layer scaling (Monin-Obukhov) can be verified. This paper describes work on the setup, calibration, installation of the sensor suite, as well as early findings from the collected data.

Keywords: Atmospheric surface layer; Optical turbulence; eddy covariance; sonic anemometer

Corresponding author; email: aperalta157@gmail.com

1 Introduction

Directed energy technology continues to be a primary interest for the scientific community and military at large due to its wide range of applications. As this technology continues to develop, knowledge of the major factors which impact directed energy systems will become increasingly important, including a deeper understanding of optical turbulence parameters. The refractive index structure parameter, C_n^2 , is the most commonly used metric to describe the strength of atmospheric turbulence. The structure parameter can be calculated directly using optical techniques, such as with a commercial scintillometer, or indirectly through measurement of the temperature structure of the atmosphere. This

paper uses eddy covariance methods to estimate the temperature structure constant, C_T^2 , using co-located measurements of velocity and sonic temperature to determine turbulent fluxes within the atmospheric surface layer. The setup and data presented comes from a near-maritime (littoral) environment, important for many naval applications of lasers.

2 Theoretical Background

Established similarity theory may be used to scale a range of quantities within the atmospheric surface layer (1; 2). In the surface layer, or the constant flux layer of the atmosphere, the turbulence structure may be scaled via five parameters: a friction velocity, the surface temperature flux, the surface flux of a conserved scalar, the buoyancy parameter, and a length scale z usually taken as the height of interest. The structure parameters for temperature or refractive index, when properly nondimensionalized, are then only functions of a nondimensional stability parameter. This scaling within the surface layer, termed Monin-Obukhov Similarity Theory (MOST), has been used successfully in a wide range of applications (3; 4; 5; 6; 7).

In Monin-Obukhov similarity theory, velocity may be scaled with the friction velocity, u_* , which is related to the shear stress and defined as

$$u_* = \left[\overline{u'w'^2} + \overline{v'w'^2} \right]^{\frac{1}{4}}, \quad (1)$$

where u' , v' , and w' are the fluctuating velocity components in the stream wise, transverse, and vertical directions, and over-bar denotes averaging. The Obukhov length scale, L , is then

$$L = - \frac{u_*^3}{k \left(\frac{g}{T} \right) \left(\overline{w'T'} \right)}, \quad (2)$$

where \overline{T} is the virtual air temperature in Kelvin, g is the gravitational constant, and k is the Von-Karman constant of 0.41. Nondimensionalization of temperature will use the turbulent temperature scale, T_* , defined as

$$T_* = -\frac{\left(\overline{w'T'}\right)}{u_*}. \quad (3)$$

Finally, using the Obukhov length and a reference height, the stability parameter $\frac{z}{L}$ is

$$\frac{z}{L} = -\frac{\left(g/\overline{T}\right)\left(\overline{w'T'}\right)}{u_*^3/kz}, \quad (4)$$

where z is, for maritime measurements, the vertical height from the waterline. This stability parameter may be interpreted as a ratio of the amount of turbulence generated from buoyancy compared to the amount of turbulence generated from shear.

Given these scaling parameters, MOST theory then allows the nondimensional scaling of turbulent quantities within the surface layer as a function of just the stability parameter. For example, the turbulent stresses σ will scale as

$$\frac{\sigma_i}{u_*} = \phi_i\left(\frac{z}{L}\right) = A_i \left[1 + B_i \left|\frac{z}{L}\right|\right]^{C_i}, \quad i = u, v, w; \quad (5)$$

where A_i , B_i , C_i , are the scaling coefficients determined from field experiment. Likewise, the temperature structure constant C_T^2 will be nondimensionalized and scaled as

$$\frac{(kz)^2 C_T^2}{T_*^2} = \phi_i\left(\frac{z}{L}\right). \quad (6)$$

Finally, from C_T^2 the Refractive Index Structure Constant, C_n^2 , can be found:

$$C_n^2 = \left(79 * 10^{-6} \left[\frac{K}{mbar}\right] \frac{P}{T^2}\right)^2 C_T^2. \quad (7)$$

3 Experiment

To determine the surface layer turbulence structure in the context of Monin Obukhov Similarity Theory, eddy covariance is used with data from an array of sonic anemometers. The setup and implementation of this technique are described below.

The location we chose to perform our surface layer analysis is at the Water Front Readiness Center’s YP (Yard Patrol) Pier, located at 38.98N, 076.46W in Annapolis, Maryland (Fig. 1). This area is east of Washington D.C. and south-south east of Baltimore, just off the northern part of the Chesapeake Bay. The sensor array is on a pier 200 meters away from any major obstruction with the majority of its view being over the Severn River. The Severn River is to the west and northwest, the Chesapeake Bay to the south and southeast, and a low coastal environmental preserve is to the northeast. The site is adjacent to a number of other environmental monitoring instruments, including a Scintec BLS450 scintillometer, which have been used previously for atmospheric optical turbulence study (8; 9)



Figure 1: Sensor array location depicting satellite imagery of Annapolis, Maryland showing where the array is located in relation to nearby popular cities and landmarks.

Eddy covariance measurements at this location are obtained via two Campbell Scientific CSAT3B sonic anemometers and one IRGASON infrared gas analyzer. The IRGASON is an *in-situ*, open-path, mid-infrared absorption analyzer integrated with a three-dimensional sonic anemometer. Its data collection center, the EC100, measures and controls the output elements of the IRGASON such as wind velocity components, sonic air temperature, ambient temperature, H_2O and CO_2 density. The sonic anemometer (CSAT3B) is an ultrasonic anemometer used for measuring sonic temperature and three-dimensional wind velocity. The sensor array described in this paper uses two CSAT3B's in order to provide a more complete profile of the atmospheric surface layer above the Severn River.

All three instruments were mounted on a 6-m tall mast at the end of the pier. The two sonic anemometers were placed as the highest and lowest sensors with the IRGASON being placed in the center due to its collection center, the EC100, creating too big a moment arm. The top sonic anemometer, with a typical height above the water of 8-m, is labeled Anemometer 1, the IRGASON is at a height of 6-m above the water, and the bottom instrument, Anemometer 2, has a height above water of 4-m. The complete instrument mast can be seen in Fig. 2. These heights will vary with the tides, which have a typical diurnal variation of approximately 1.3-m.

The orientation of the instruments is shown in Fig. 3. The vertical sensor array is facing 166° from true north, or approximately South-South East. The positive x-axis for each sonic anemometer and IRGASON corresponds to flow into the shaft of the instrument, therefore the u velocity component will be oriented to flow at 346° , while w is up. All wind velocity readings are scaled to range from 0° to 360° , and are reported as wind vectors and not meteorological wind direction.



Figure 2: The sensor array overlooking the Severn River.



Figure 3: Sensor orientation and wind velocity angle readings compared to compass rose.

4 Data Collection and Conditioning

To program, read, and store the IRGASON and CSAT3B's data, the CR1000X data logger was used, Fig. 4. This data logger has a central-processing unit, analog and digital measurement inputs, analog and digital outputs, and onboard memory. An operating system coordinates these functions along with the data logger's onboard clock and programming application. It measures the IRGASON and CSAT3B's electrical response, drives their communications, and reduces their data to statistical values formatted in a table. The CR1000X is programmable using Loggernet, a software package capable of programming,

communication, and retrieving data between PCs and data loggers.



Figure 4: The field setup of the CR1000X data logger used to program and store sensor data.

The CR1000X programmed the IRGASON and sonic anemometers in this sensor array to receive data at 40 Hz (25 ms). The data logger runs each sensor over a period of 24 hours and stores each output table onto a 16 Gb micro SD card. Each data table has approximately 3.45 million records of data, a data table example can be seen with Fig. 5. To further analyze the data, the SD card contents are converted and read into Matlab R2020a.

TIME	RECORD	Ux	Uy	Uz	Ts	diag_sonic	CO2	H2O	diag_gpa	amb_temp	amb_press	CO2_sig_strength	H2O_sig_strength	CO2_fest_Ux_1	Ux_1	Uz_1	Ts_1	diag_si	
2021-01-01 00:00:00.000	111218065	-3.204739	0.2861075	-0.4679564	5.036119	0	839.4121	3.137725	0	4.129679	103.598	0.9623506	0.9576668	841.6478	-3.702384	-0.4573061	-1.114957	5.120128	0
2021-01-01 00:00:00.005	111218066	-3.358498	0.227175	-0.449378	5.009306	0	839.4191	3.138285	0	4.129679	103.596	0.9623524	0.9576674	841.6409	-3.729348	-0.4355039	-1.111381	5.105311	0
2021-01-01 00:00:00.010	111218067	-3.126707	0.522475	-0.3989528	5.039829	0	839.5104	3.138236	0	4.129679	103.5988	0.9623753	0.9576781	841.7508	-3.800596	-0.5768693	-1.057944	5.095552	0
2021-01-01 00:00:00.015	111218068	-3.214945	0.698619	-0.409924	5.047669	0	839.5206	3.138115	0	4.129679	103.5988	0.9623787	0.9576796	841.7753	-3.733994	-0.6570055	-0.987474	5.092611	0
2021-01-01 00:00:00.020	111218069	-3.045969	0.6478865	-0.4367068	4.985376	0	839.5352	3.139262	0	4.129679	103.5962	0.9623512	0.9576612	841.7432	-3.519003	-0.6371209	-0.8288238	5.10198	0
2021-01-01 00:00:00.025	111218070	-3.044414	0.5311048	-0.403104	4.956649	0	839.562	3.140254	0	4.129679	103.5962	0.9623372	0.9576519	841.7511	-3.464139	-0.5652468	-0.7249812	5.097723	0
2021-01-01 00:00:00.030	111218071	-3.041317	0.4622981	-0.4198464	4.975665	0	839.6371	3.139952	0	4.129679	103.5957	0.9623472	0.9576588	841.839	-3.559242	-0.5031855	-0.6757	5.09846	0
2021-01-01 00:00:00.035	111218072	-2.98543	0.4701918	-0.4249496	5.014465	0	839.6412	3.139313	0	4.129679	103.5957	0.9623628	0.9576684	841.8663	-3.60726	-0.5217808	-0.7288775	5.10496	0
2021-01-01 00:00:00.040	111218073	-2.961157	0.4037887	-0.4204264	5.030835	0	839.6052	3.139433	0	4.129679	103.5973	0.9623688	0.9576705	841.8755	-3.570031	-0.5579051	-0.7714171	5.11588	0
2021-01-01 00:00:00.045	111218074	-2.824866	0.378725	-0.4035728	5.039633	0	839.6004	3.139999	0	4.129679	103.5973	0.9623596	0.9576646	841.8729	-3.541185	-0.5253464	-0.7105966	5.116933	0
2021-01-01 00:00:00.050	111218075	-2.783958	0.4502239	-0.4357619	5.050067	0	839.5896	3.139999	0	4.129679	103.5972	0.9623563	0.9576625	841.8329	-3.499857	-0.4396311	-0.5632985	5.095656	0
2021-01-01 00:00:00.055	111218076	-2.793124	0.4709729	-0.4267328	5.030229	0	839.5663	3.139683	0	4.129679	103.5972	0.9623667	0.9576681	841.8009	-3.412394	-0.4483546	-0.3996264	5.093772	0
2021-01-01 00:00:00.060	111218077	-2.919901	0.3898075	-0.3792825	5.052276	0	839.5352	3.139658	0	4.129679	103.5975	0.9623777	0.9576743	841.7997	-3.263027	-0.5474007	-0.5007879	5.081904	0
2021-01-01 00:00:00.065	111218078	-2.992854	0.3209465	-0.3444551	5.058115	0	839.5695	3.140078	0	4.129679	103.5975	0.9623702	0.9576728	841.8369	-3.258109	-0.5660901	-0.5051885	5.099946	0
2021-01-01 00:00:00.070	111218079	-3.015789	0.3710015	-0.2521392	5.085904	0	839.5968	3.140008	0	4.129679	103.5995	0.9623506	0.9576715	841.8643	-3.394868	-0.4949999	-0.5663344	5.097988	0
2021-01-01 00:00:00.075	111218080	-2.97977	0.4522279	-0.2120261	5.047966	0	839.6053	3.141538	0	4.129679	103.5995	0.9623494	0.9576727	841.8506	-3.481656	-0.4757286	-0.6707862	5.093507	0
2021-01-01 00:00:00.080	111218081	-2.926208	0.5147922	-0.2137728	4.994267	0	839.6096	3.14117	0	4.129679	103.5997	0.9623618	0.9576721	841.9031	-3.526118	-0.5600838	-0.8023324	5.088372	0
2021-01-01 00:00:00.085	111218082	-2.908004	0.5093933	-0.2451133	4.993062	0	839.7389	3.144356	0	4.129679	103.5997	0.9623697	0.9576707	841.9714	-3.541367	-0.6615274	-0.7751362	5.082775	0
2021-01-01 00:00:00.090	111218083	-2.846004	0.324885	-0.2960868	4.996162	0	839.7913	3.141799	0	4.129679	103.5983	0.9623759	0.9576719	842.0056	-3.596881	-0.7690947	-0.6021922	5.063196	0
2021-01-01 00:00:00.095	111218084	-2.829101	0.1451175	-0.3123687	4.991055	0	839.7312	3.140223	0	4.129679	103.5983	0.9623719	0.957673	841.9427	-3.627861	-0.8031599	-0.505996	5.04331	0
2021-01-01 00:00:00.100	111218085	-2.839032	-0.1774952	-0.2797109	4.990113	0	839.6629	3.141179	0	4.129679	103.5945	0.9623555	0.9576629	841.8727	-3.58144	-0.7692859	-0.4397221	5.022995	0
2021-01-01 00:00:00.105	111218086	-2.859441	-0.2513071	-0.161719	4.992427	0	839.705	3.141672	0	4.129679	103.5945	0.9623501	0.9576549	841.9202	-3.495431	-0.7471255	-0.4016983	5.020911	0
2021-01-01 00:00:00.110	111218087	-2.782794	-0.3313576	-0.2559724	5.013719	0	839.813	3.141806	0	4.129679	103.5985	0.9623538	0.9576742	842.038	-3.438089	-0.8366593	-0.3645177	5.042638	0
2021-01-01 00:00:00.115	111218088	-2.75147	-0.3691241	-0.2960507	5.021086	0	839.8179	3.141968	0	4.129679	103.5985	0.9623564	0.9576519	842.0482	-3.512794	-0.9980905	-0.3912699	5.009696	0
2021-01-01 00:00:00.120	111218089	-2.765658	-0.3694073	-0.2835297	5.020063	0	839.7763	3.141603	0	4.129679	103.5943	0.9623516	0.9576533	842.0087	-3.478061	-1.021761	-0.420253	5.077263	0
2021-01-01 00:00:00.125	111218090	-2.720719	-0.121699	-0.1677931	5.010985	0	839.7854	3.143873	0	4.129679	103.5943	0.9623471	0.957651	841.9797	-3.718179	-1.089991	-0.3822658	5.077228	0
2021-01-01 00:00:00.130	111218091	-2.611221	-0.0159749	-0.281356	4.957829	0	839.7182	3.142521	0	4.129679	103.5964	0.9623529	0.9576561	841.9154	-3.693285	-1.078187	-0.2212929	5.097918	0
2021-01-01 00:00:00.135	111218092	-2.603052	-0.0722385	-0.4550661	4.963024	0	839.6932	3.141636	0	4.140137	103.5964	0.9623621	0.9576644	841.8875	-3.684335	-1.052881	-0.1339071	5.094218	0
2021-01-01 00:00:00.140	111218093	-2.738443	0.02887098	-0.482981	4.993999	0	839.6722	3.141496	0	4.140137	103.5951	0.9623751	0.9576718	841.8856	-3.663667	-0.863131	-0.0599366	5.096416	0
2021-01-01 00:00:00.145	111218094	-2.849796	0.209407	-0.293308	5.00109	0	839.6672	3.14267	0	4.140137	103.5951	0.9623712	0.9576794	841.8835	-3.616903	-0.6920023	-0.0003661	5.010109	0
2021-01-01 00:00:00.150	111218095	-2.8232	0.2593143	-0.2923335	4.96931	0	839.6588	3.141813	0	4.140137	103.5952	0.9623524	0.9576567	841.8569	-3.544302	-0.5658085	-0.0282085	5.122749	0
2021-01-01 00:00:00.155	111218096	-2.777671	0.1860117	-0.0849984	4.963123	0	839.6791	3.140762	0	4.140137	103.5952	0.9623479	0.9576557	841.8737	-3.502805	-0.5575067	-0.0686935	5.147573	0
2021-01-01 00:00:00.160	111218097	-2.844709	0.1502628	-0.2076181	5.008866	0	839.7708	3.141589	0	4.140137	103.5967	0.9623553	0.9576585	841.963	-3.370207	-0.5197048	-0.0619285	5.12956	0
2021-01-01 00:00:00.165	111218098	-2.919224	0.36139	-0.1216293	5.027854	0	839.7874	3.142871	0	4.140137	103.5967	0.9623577	0.9576573	842.0206	-3.26651	-0.4518861	-0.0747881	5.121662	0
2021-01-01 00:00:00.170	111218099	-2.80217	0.3801451	-0.0380824	4.986697	0	839.7035	3.142748	0	4.140137	103.5944	0.9623502	0.9576542	841.9105	-3.263449	-0.4039311	-0.209178	5.00012	0
2021-01-01 00:00:00.175	111218100	-2.754139	0.0897981	-0.0104389	4.956602	0	839.6545	3.14147	0	4.140137	103.5944	0.962348	0.9576562	841.8453	-3.323697	-0.264959	-0.3482028	5.112306	0
2021-01-01 00:00:00.180	111218101	-2.996128	-0.2527891	-0.241583	4.97854	0	839.6886	3.141426	0	4.140137	103.595	0.9623555	0.9576495	841.8906	-3.221407	-0.1757975	-0.408084	5.062228	0
2021-01-01 00:00:00.185	111218102	-2.836669	-0.0720711	-0.235706	4.951777	0	839.7406	3.142614	0	4.140137	103.595	0.9623576	0.9576493	841.9694	-3.025271	-0.0611912	-0.3020294	5.071785	0
2021-01-01 00:00:00.190	111218103	-2.793075	0.4252982	-0.05659691	5.034939	0	839.7861	3.143095	0	4.140137	103.5958	0.9623461	0.9576555	842.0238	-2.908858	-0.1493786	-0.1438227	5.085193	0

Figure 5: Table output showing the sensor's collected data from January 1st.

To analyze the collected three-dimensional velocity and sonic temperature data, the outputs were sorted into 30 minute stationary intervals. Data conditioning included outlier identification and linear detrending (see Fig. 6). The fluctuating components, $u' = u - \bar{u}$, where \bar{u} is the mean from each 30 minute interval, were calculated from the detrended data. The quantities from Section 2 were calculated on each 30 minute interval over the course of 7 days, 01 Jan 2021 - 08 Jan 2021. The figures below present ensemble averages across each of the seven days.

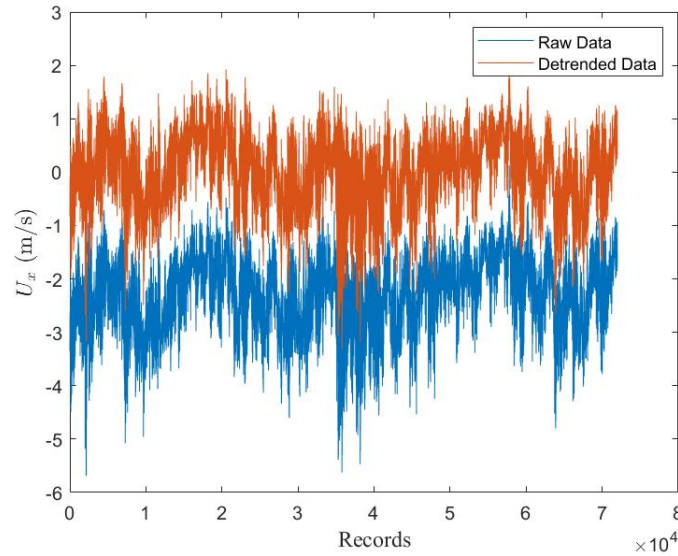


Figure 6: Example of linear detrending.

5 Results and Discussion

The following figures provide representative examples of the quantities that may be obtained from this sensor suite. Figure 7 shows the magnitudes of the velocity for each instrument as a function of time of day. The figure shows higher winds typical in the afternoon, and the linear velocity profile in this region of the boundary layer is also visible. Additionally, Figure 8 shows wind angle vs. time of day. As expected, there is little variation in wind direction with height, although the general wind direction for this week is not typical for the region.

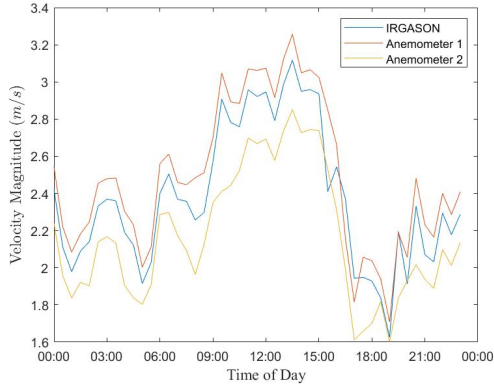


Figure 7: Velocity magnitudes.

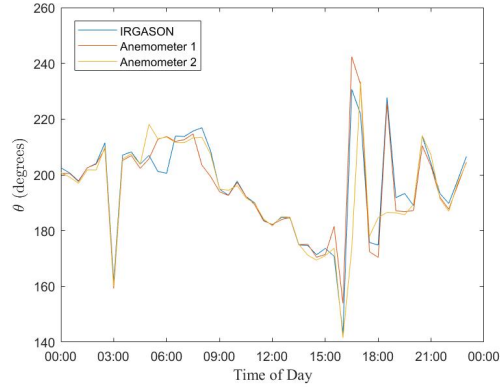


Figure 8: Velocity angles within the orientation of the sensor array.

The friction velocity, or shear velocity, is related to the level of turbulence in the boundary layer. Figure 1 shows the turbulence fluxes typically increase in the afternoon and are lower at night. The turbulent temperature (Fig. 10), on the other hand, has a minimum in the late morning and peaks in the late afternoon.

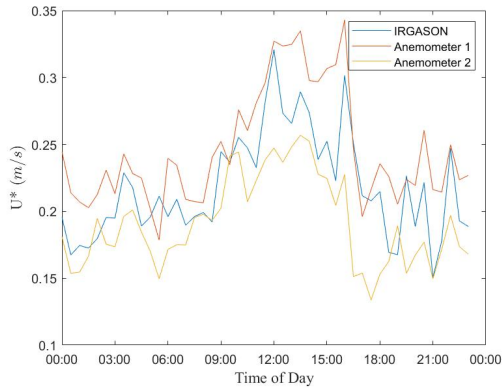


Figure 9: Friction velocity.

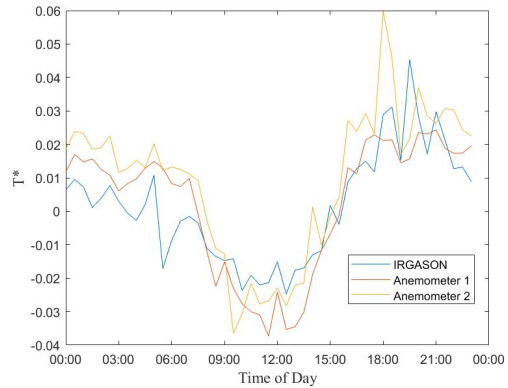


Figure 10: Turbulent temperature.

Figure 11 depicts the regions of the boundary layer which are unstable. The overall trend throughout the week shows the boundary layer becoming stable or neutral through the course of the morning then becoming unstable in the afternoon and evening. The above figures are all based on preliminary data gathered from the first week of January. The prevailing wind direction during this week was unusual, and there was no conditioning

based on wind speed or direction. The future work of this project is to continue to gather data to show the long term variations of the Severn River boundary layer, and to produce Monin Obukhov scaling coefficients for C_T^2 and C_n^2 for this environment.

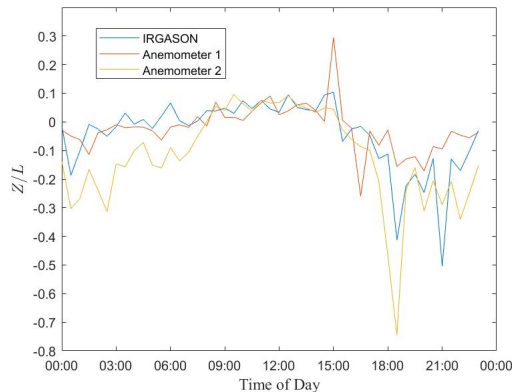


Figure 11: Stability parameter of the analyzed layer.

6 Conclusions

This paper presents early data from a new near-maritime sensor suite. Because of the unique and secure location, these instruments will provide long-term data that will assist in the study of optical turbulence, including the ability to assess seasonal variations and infrequent extreme events. For discussion or data access please contact the authors.

Acknowledgements

The authors acknowledge the generous support from ONR and DE-JTO.

References

- [1] Wyngaard, J.C., *Turbulence in the Atmosphere*. Cambridge Press, 2010.
- [2] J. C. Wyngaard, Y. Izumi, Stuart A. Collins Jr. “Behavior of the Refractive-Index-Structure Parameter near the Ground.” *Journal of the Optical Society of America*, 61 (12), 1971.
- [3] T.A. Paco, M.I. Ferreira, and N. Conceicao. “Peach orchard evapotranspiration in a sandy soil: comparison between eddy covariance measurements and estimates by the FAO 56 approach.” *Agr. Water Mgmt.* 85, 2006.

- [4] M.L. Goulden, J.W. Munger, S.-M. Fan, B.C. Daube, and S.C. Wofsy. “Measurements of carbon sequestration by long-term eddy covariance: methods and a critical evaluation of accuracy.” *Global Change Bio.* 2, 1996.
- [5] E. Velasco, S. Pressley, R. Grivicke, et al., “Eddy covariance flux measurements of pollutant gases in urban Mexico City.” *Atmos. Chem. Phys.* 9, 2009.
- [6] Dan Li, Elie Bou-Zeid, Henk A. R. De Bruin. “Monin-Obukhov Similarity Functions for the Structure Parameters of Temperature and Humidity.” *Boundary-Layer Meteorol.* 2011.
- [7] Arindam Singha, Reza Sadr. “Characteristics of Surface Layer Turbulence in Coastal Area of Qatar.” *Environmental Fluid Mechanics*, 2012.
- [8] C. Jellen, J. Burkhardt, C.J. Brownell, and C. Nelson, “Machine learning informed predictor importance measures of environmental parameters in maritime optical turbulence.” *Applied Optics*, 59 (21), 2020.
- [9] C. Jellen, C. Nelson, C. Brownell, J. Burkhardt, and M. Oakley, “Measurement and analysis of atmospheric turbulence in a near-maritime environment.” *IOP SciNotes*, 1 (2), 2020.